THE IMAGING X-RAY POLARIMETRY EXPLORER (IXPE)

An overview of the history of X-ray polarimetry and IXPE - the mission and its science

Martin C. Weisskopf
On behalf of the IXPE team

TORINO, April 6, 2017

(Linear) X-ray polarimetry is difficult

- One does not expect all astrophysical systems to be strongly polarized.

- Instruments typically not fully sensitive to polarization

- Measured parameter is positive definite – i.e. one always measures something, even in the absence of a polarized source

Rocket history

- 1968 Aerobee 150
  - Sco X-1 upper limit
- 1969 Aerobee 150
  - Crab upper limit
- 1971 Aerobee 350
  - Crab detection!
    - P = 15% ± 5%
    - φ = 156° ± 10°

Rocket 17.09

- Two instruments
  - Lithium scattering polarimeter
  - 4 Bragg crystal polarimeters

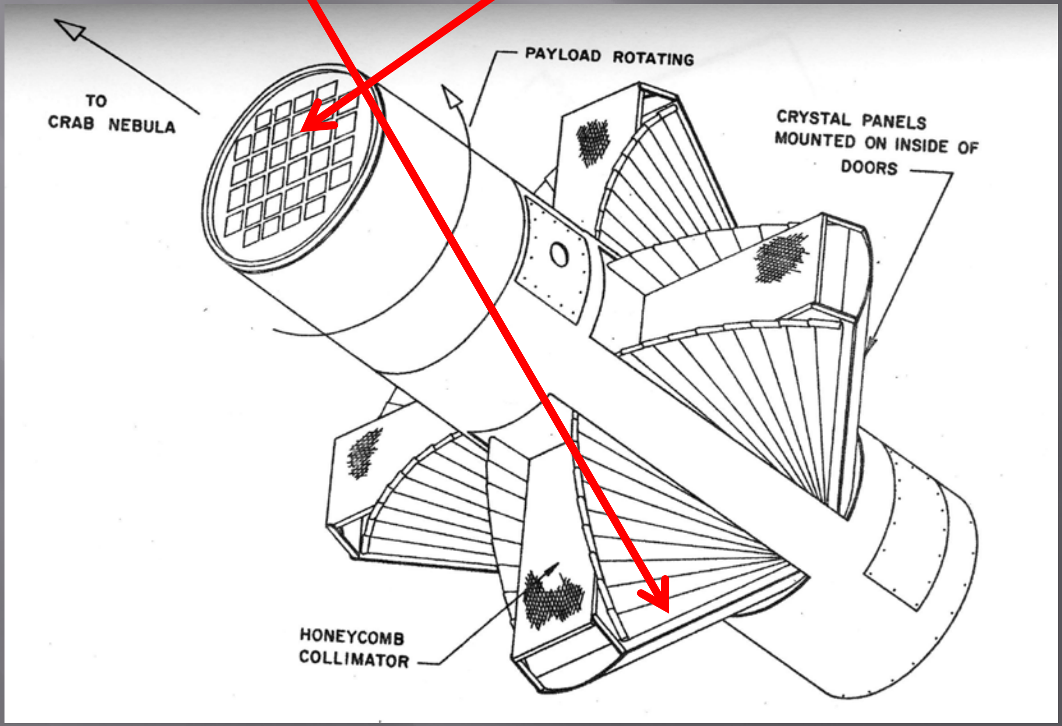

On to the satellite experiment

- 1975 OSO-8 crystal polarimeter
  - Precision measurement of integrated Crab Nebula polarization at 2.6 keV
    - $\Pi = 19\% \pm 1\%$
    - $\varphi = 156^\circ \pm 2^\circ$ (NNE) agrees with optical

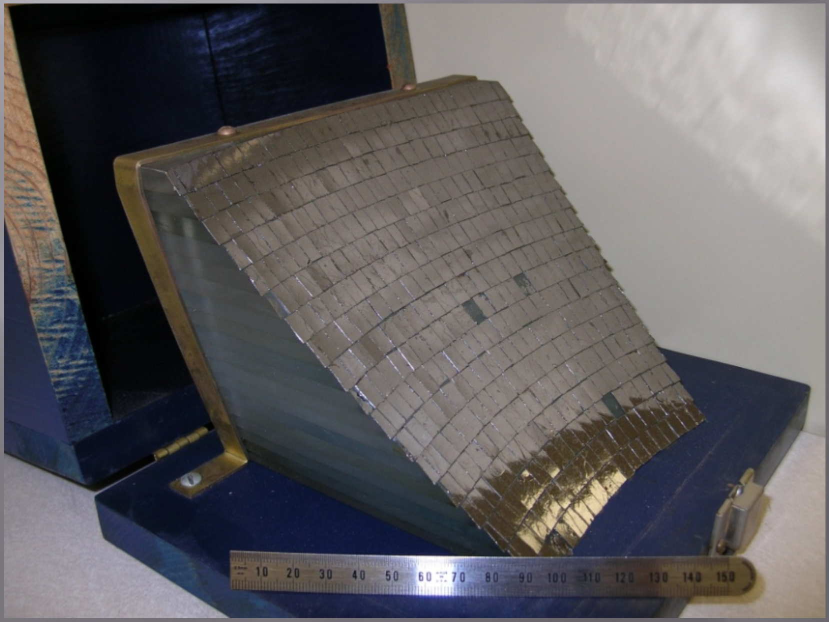

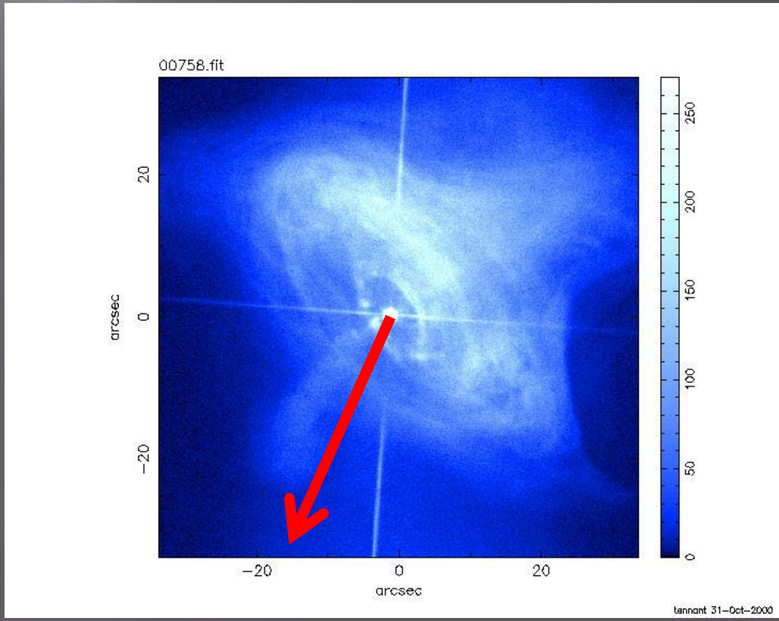

IXPE

- Three redundant telescope-detector systems
- Gas pixel electron-tracking detectors developed in Italy
- Replicated X-ray telescopes with <30 arcsecond angular resolution (half-power diameter) developed at MSFC

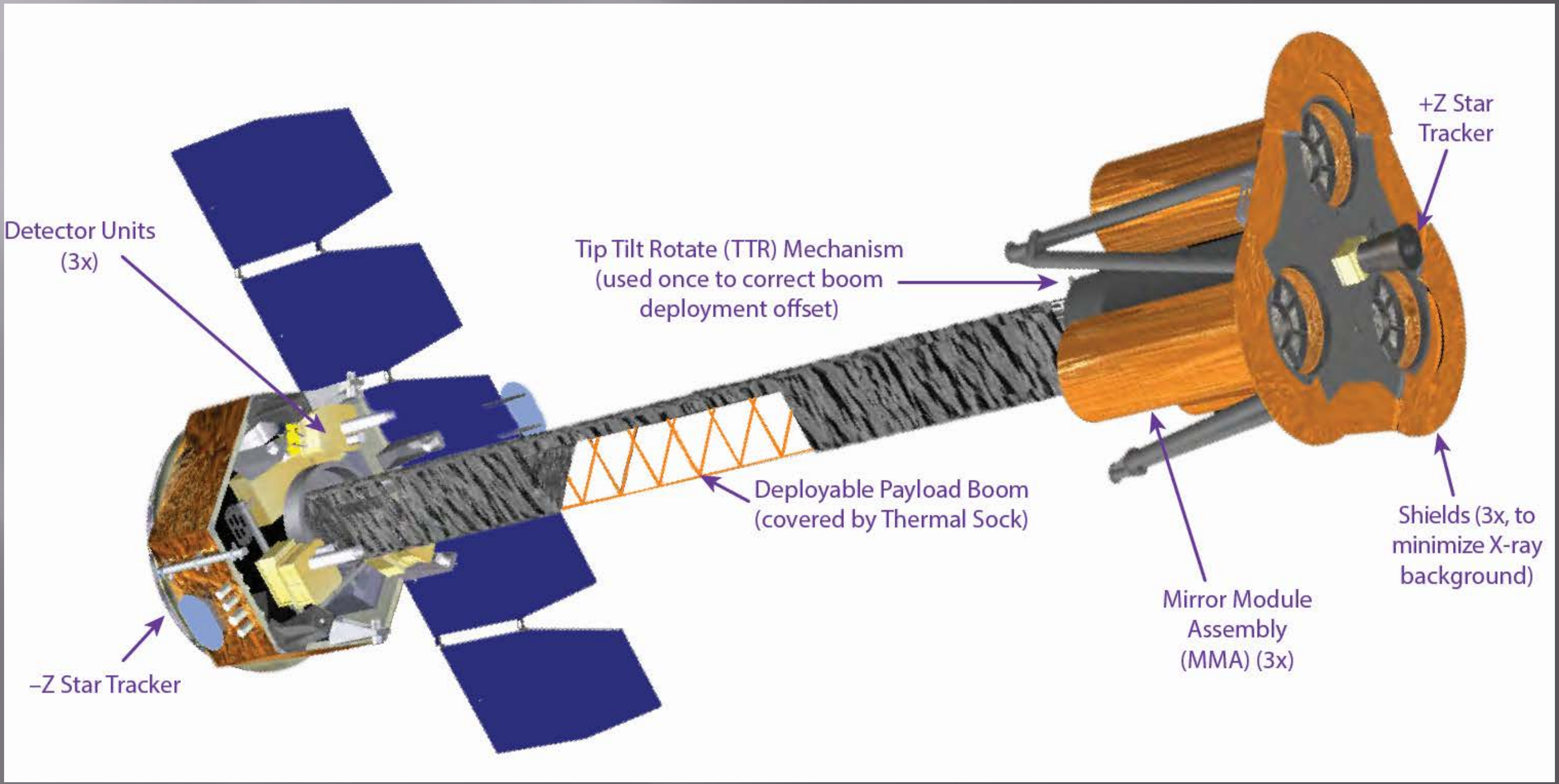

Participating Institutions & Roles

- NASA/MSFC- PI Team, project management, systems engineering, technical oversight, telescope fabrication, X-ray calibration, science operations, data analysis
- Istituto di Astrofisica e Planetologia Spaziale/Istituto Nazionale di Astrofisica (IAPS/INAF, Rome) & Istituto Nazionale di Fisica Nucleare (INFN, Pisa & Torino) – Polarization-sensitive detectors & electronics, detector calibration & data analysis
- Agenzia Spaziale Italiana (ASI) – Malindi Ground Station
- Ball Aerospace – Spacecraft, Payload Structure, Payload and Observatory I&T
- Laboratory for Astronomy & Space Physics (Boulder) – Mission Operations
- Stanford University & University Roma Tre – Theory
- McGill University & MIT – Co-Chair SWG & Co-Is

Science Team

Martin C. Weisskopf (MSFC) – PI
Luca Baldini (INFN) – Co-I
Ronaldo Bellazzini (INFN,) – Co-I and Italian Co-PI
Enrico Costa (IAPS/INAF) – Senior Co-I
Ronald Elsner (MSFC) –Co-I & Science Systems Eng.
Victoria Kaspi (McGill) – Co-I & SWG Co-Chair
Jeffery Kolodziejczak (MSFC) – Co-I & Calibration Scientist
Luca Latronico (INFN) – Co-I
Herman Marshall (MIT) – Co-I
Giorgio Matt (Univ Roma Tre) – Co-I & Theory
Fabio Muleri (IAPS/INAF) – Co-I
Stephen O'Dell (MSFC) – Co-I & Project Scientist
Brian Ramsey (MSFC) – Co-I, Deputy PI, Payload Scientist
Roger Romani (Stanford) – Co-I & Theory
Paolo Soffita (IAPS/INAF) – Co-I and PI for Italian effort
Allyn Tennant (MSFC) – Co-I & Science Data Ops Lead

Collaborators (11 Countries)

W. Baumgartner, A. Brez, N. Bucciantini,
E. Churazov, S. Citrano, E. Del Monte,
N. Di Lalla, I. Donnarumma, M. Dovčiak,
Y. Evangelista, S. Fabiani, R. Goosmann,
S. Gunji, V. Karas, M. Kuss,
A. Manfreda, F. Marin, M. Minuti,
N. Omodei, L. Pacciani, G. Pavlov,
M. Pesce-Rollins, P.-O. Petrucci, M. Pinchera,
J. Poutanen, M. Razzano, A. Rubini,
M. Salvati, C. Sgrò, F. Spada,
G. Spandre, L. Stella, R. Sunyaev,
R. Taverna, R. Turolla,
K. Wu, S. Zane, D.

Electron tracking - 1

- **The direction of the K-shell photoelectron is determined by the electric vector and the direction of the incoming photon**

$$\frac{d\sigma}{d\Omega} = f(\zeta) r_0^2 Z^5 \alpha_0^4 \left(\frac{1}{\beta}\right)^{7/2} 4\sqrt{2}\sin^2\theta\cos^2\varphi$$

$$\textbf{where } \boldsymbol{\beta} \equiv \frac{\boldsymbol{E}}{\boldsymbol{mc^2}} = \frac{\boldsymbol{h\nu}}{\boldsymbol{mc^2}}$$

Electron tracking - 2

- **Optical Imaging Chamber**
  - **Austin & Ramsey 1992**

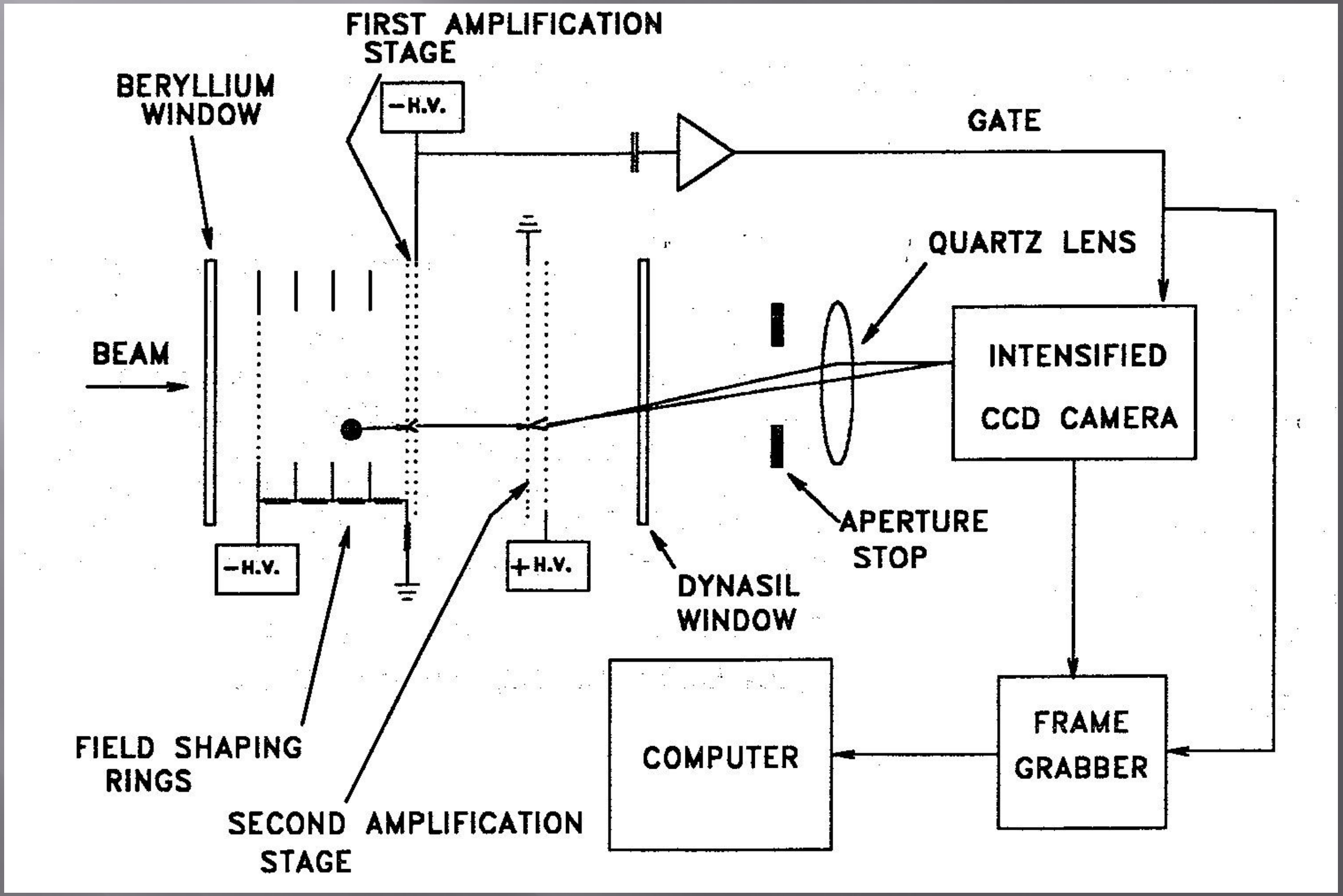

Electron tracking - 3

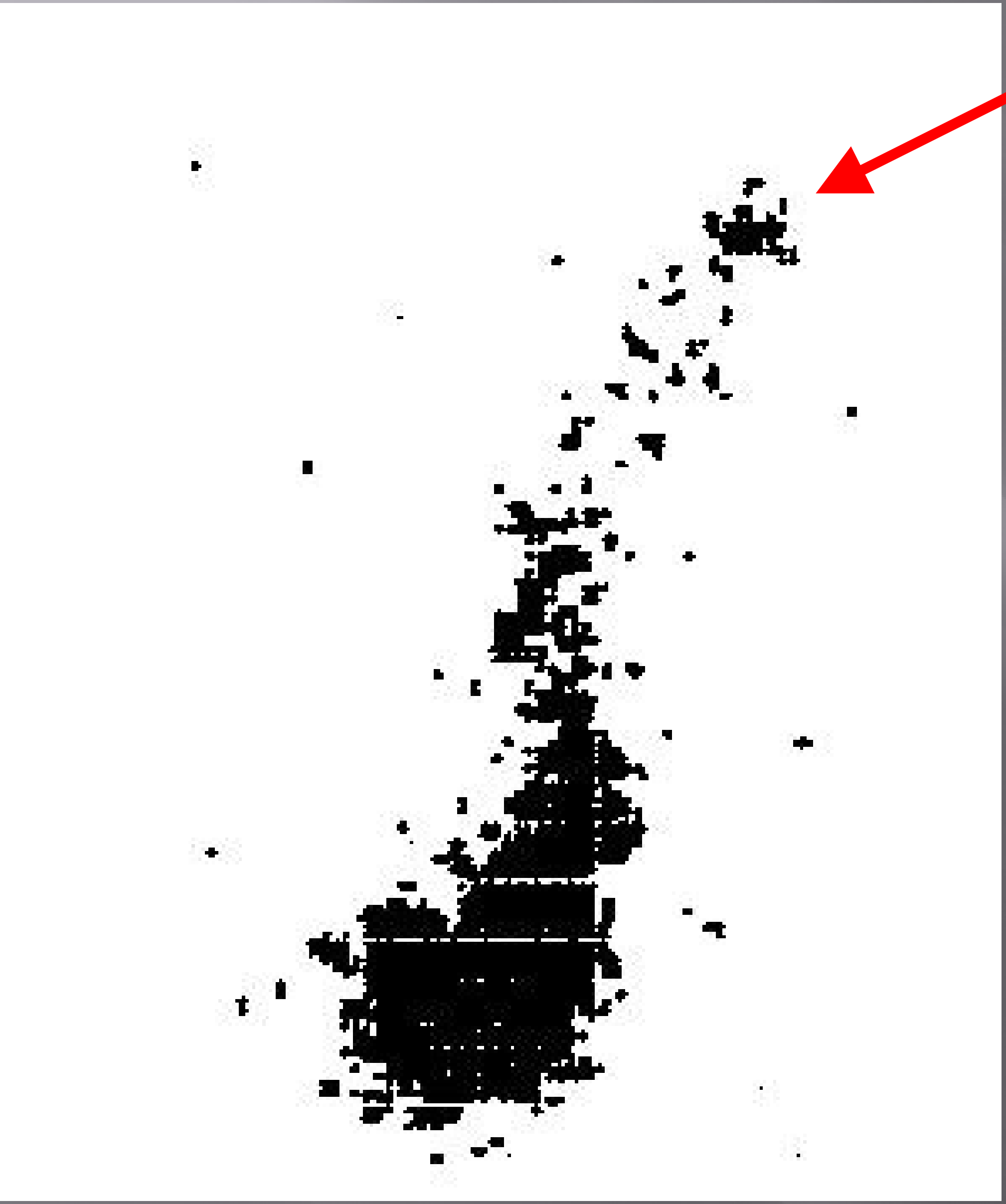

Site of initial ionization produced by 54 keV X-ray and the Auger electron cloud

- 2 atm:
  - argon (90%) ,
  - methane (5%)
  - trimethyamine (5)%
- Track is 14 mm long

The IXPE detectors

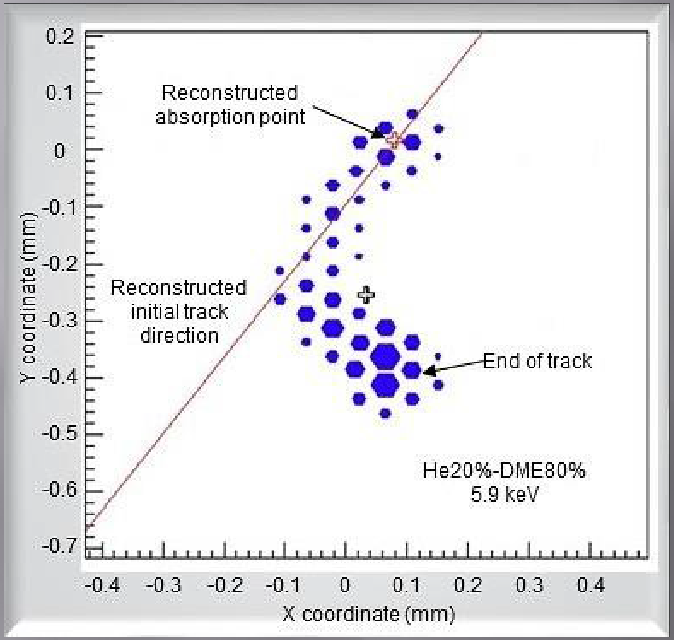

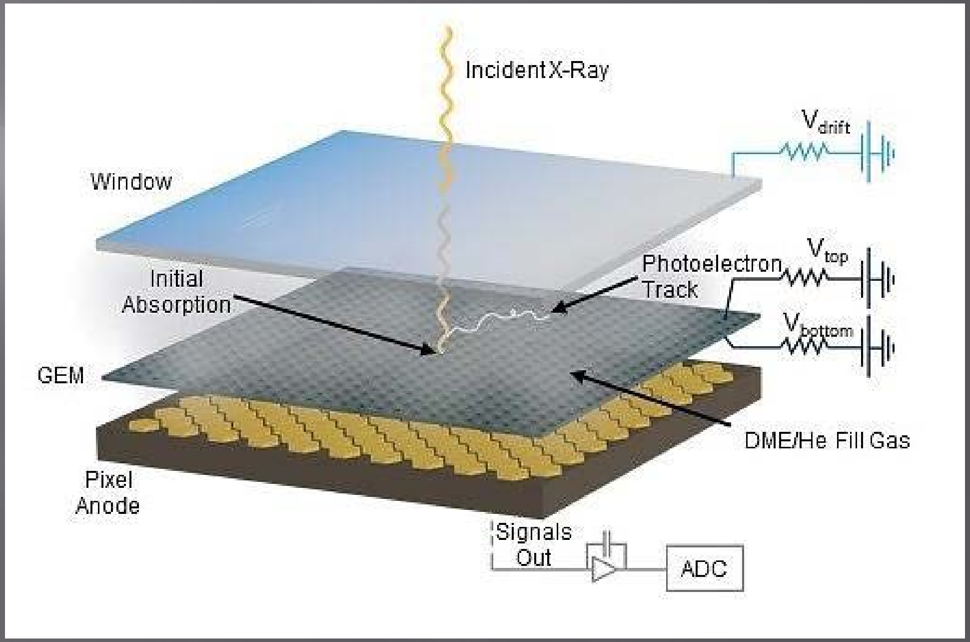

The distribution of the photoelectron directions determines the degree of polarization and the position angle

The polarization sensitive detectors

Parameter	Value
Sensitive area	15 mm × 15 mm
Fill gas and composition	He/DME (20/80) @ 1 atm
Detector window	50-µm thick beryllium
Absorption and drift region depth	10 mm
GEM (gas electron multiplier)	copper-plated 50-µm liquid-crystal polymer
GEM hole pitch	50 µm triangular lattice
Number ASIC readout pixels	300 × 352
ASIC pixelated anode	Hexagonal @ 50-µm pitch
Spatial resolution (FWHM)	≤ 123 µm (6.4 arcsec) @ 2 keV
Energy resolution (FWHM)	0.54 keV @ 2 keV ($\propto \sqrt{E}$)

The Modulation Factor - 1

Measurements of the detector modulation with a 100%-polarized beam at 3.7 keV

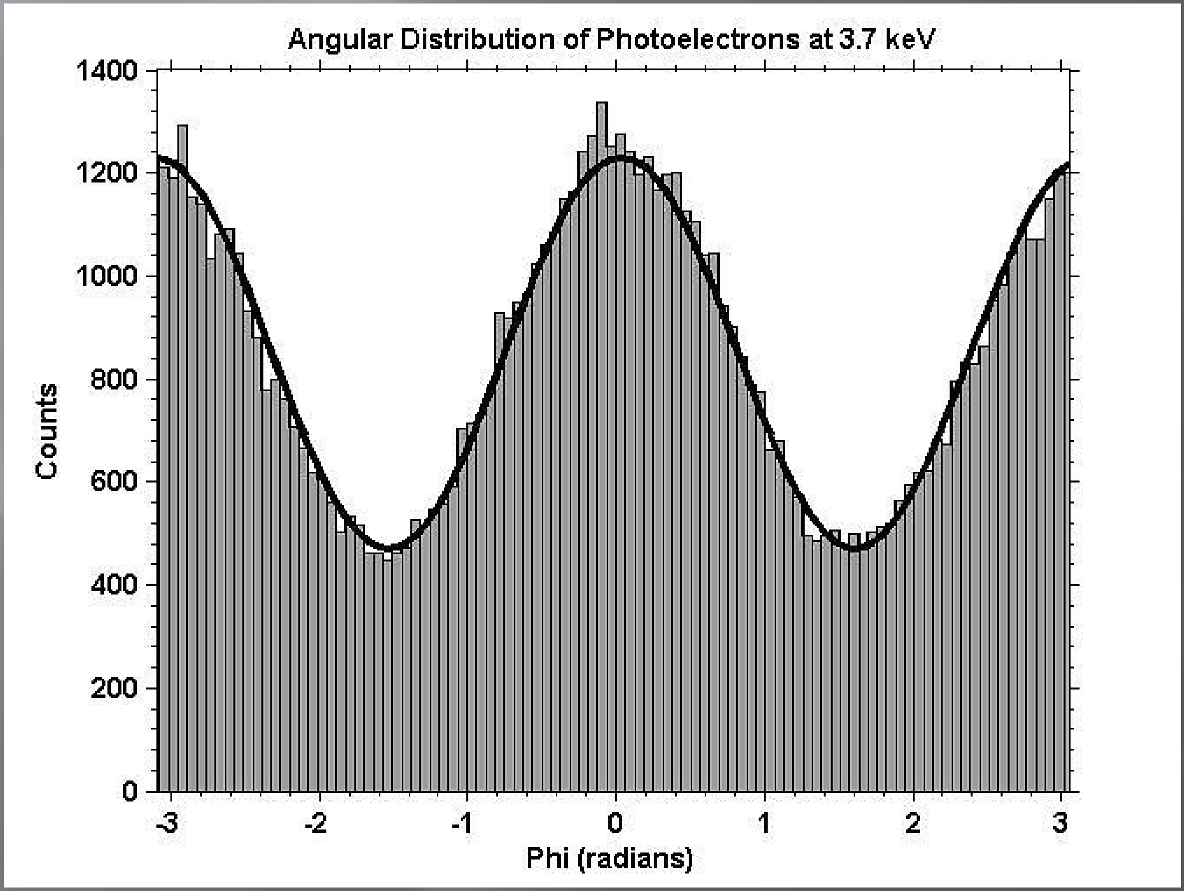

The Modulation Factor - 2

Measurements of the detector modulation with an un-polarized beam at 3.7 keV

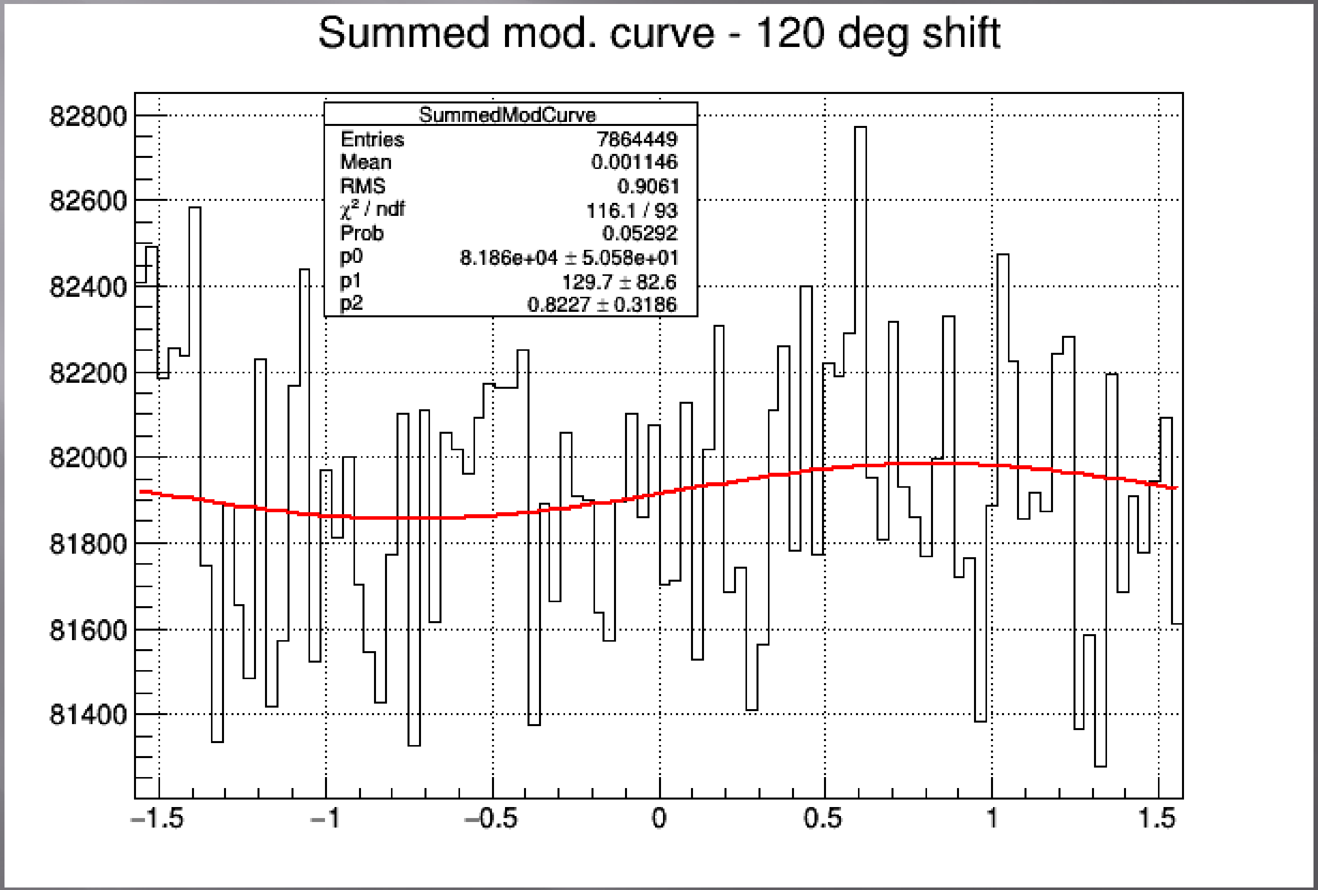

The Modulation Factor -3

Modulation factor as a function of energy
Comparison to simulations

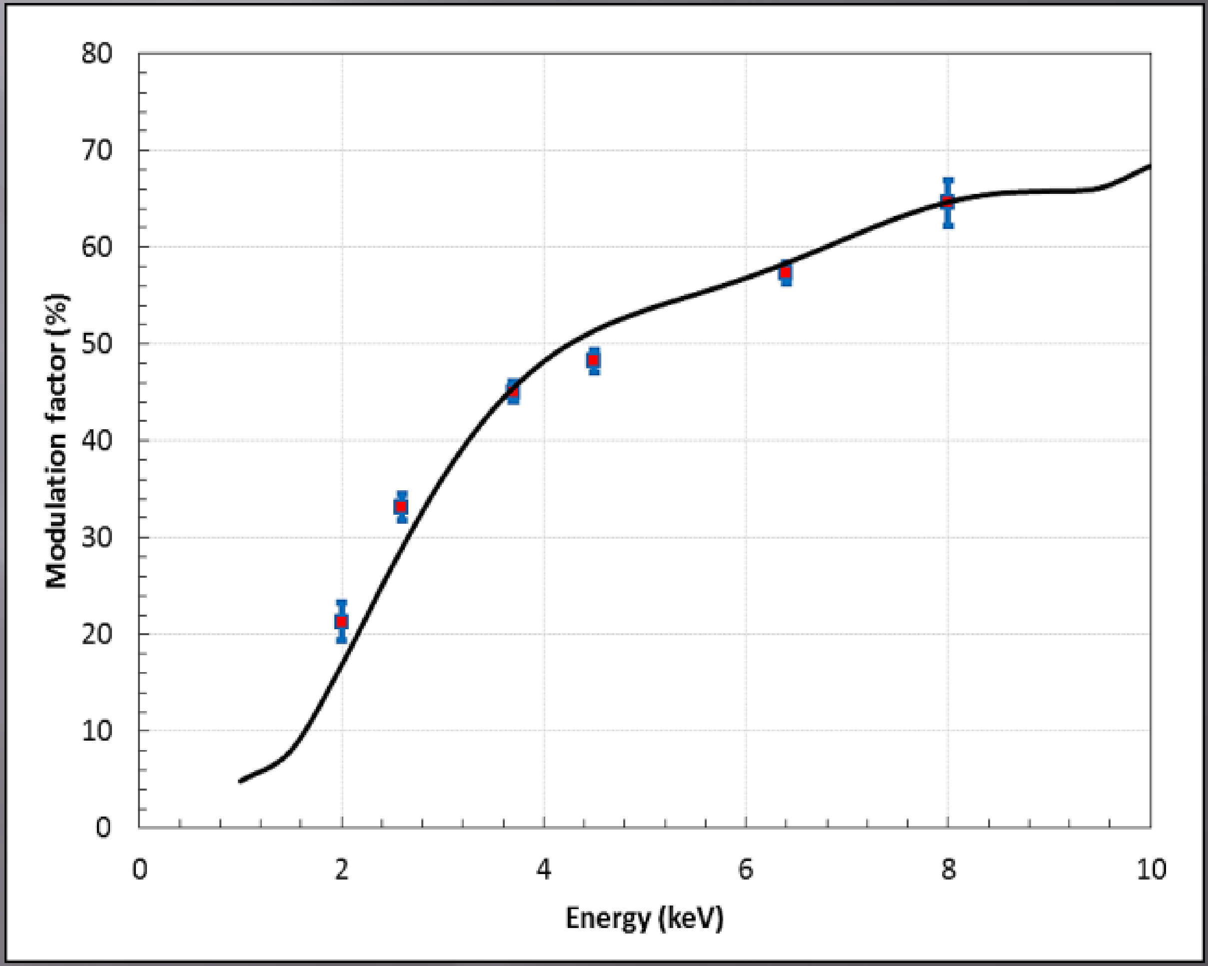

The X-ray telescopes

An ART-XC flight module in its support frame (rear view)

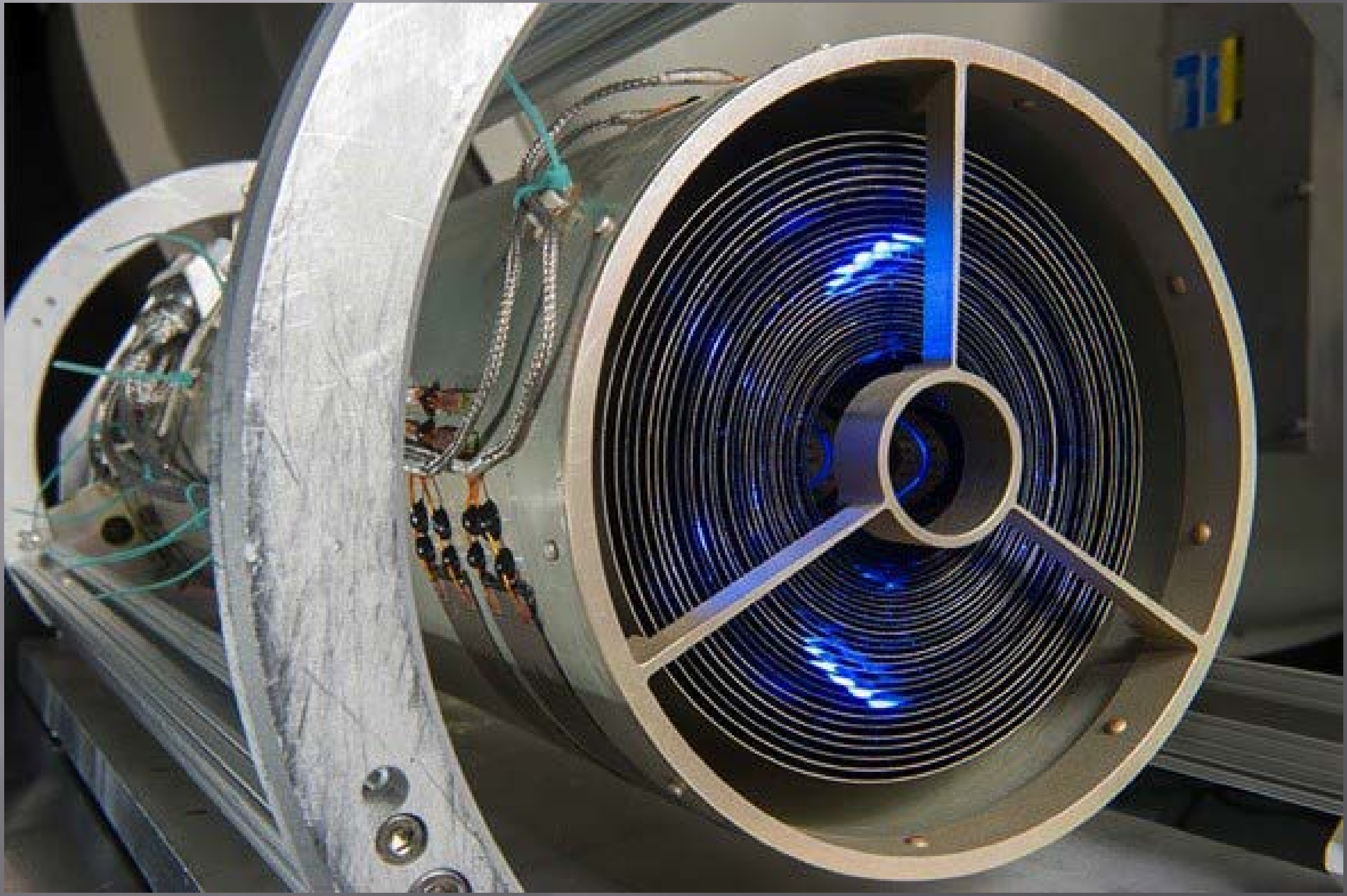

The IXPE X-ray mirror modules

Parameter	Value
Number of mirror modules	3
Number of shells per mirror module	24
Focal length	4000 mm
Total shell length	600 mm
Range of shell diameters	162–272 mm
Range of shell thicknesses	0.16–0.26 mm
Shell material	Electroformed nickel–cobalt alloy
Effective area per mirror module	230 cm^2 (@ 2.3 keV); >240 cm^2 (3–6 keV)
Angular resolution (HPD)	≤ 25 arcsec
Field of view (detector limited)	12.9 arcmin square

The Energy Response

Modulation factor × square root of the effective area versus energy

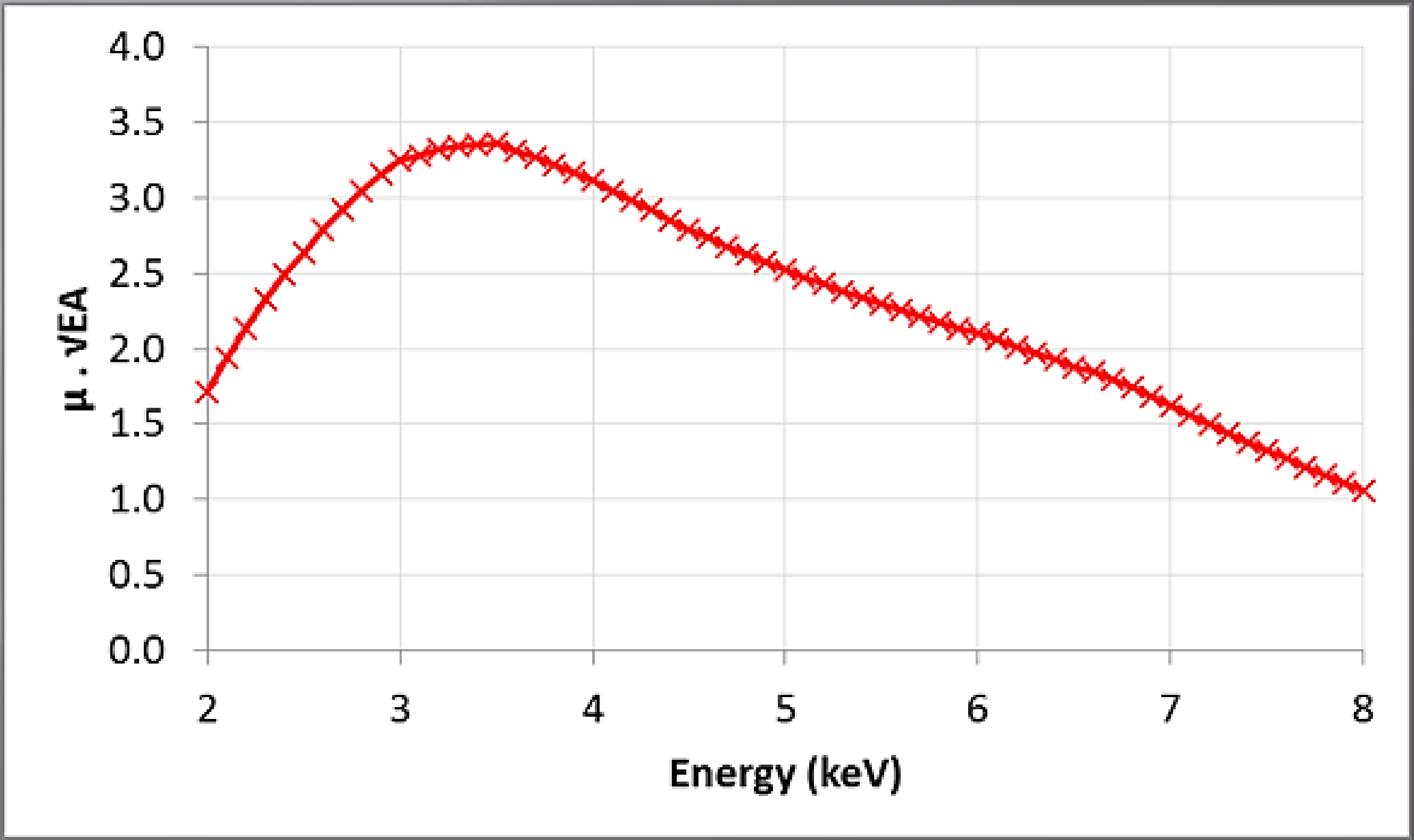

End-to-end flow from detected photon to scientific data products

IXPE

Photons to Data Products

Fundamental new measurements

- **Obtain X-ray polarimetric images of an AGN core and jet**
- **Exploit imaging polarimetry to infer past activity of Sgr A***
- **Map magnetic field of X-ray-emitting regions in Pulsar Wind Nebulae and in shell-type Supernova Remnants**
- **Perform phase-resolved polarimetry of rotation-powered pulsars using imaging to reduce nebular background**
- **Explore Magnetar physics and vacuum birefringence**
- **Obtain energy-resolved polarimetry of AGN and microquasars to test models and assess black-hole spin**
- **Perform phase- and energy-resolved polarimetry of accreting X-ray pulsars to test emission models**

Sensitivity

Time to reach a minimum detectable polarization as a function of source flux

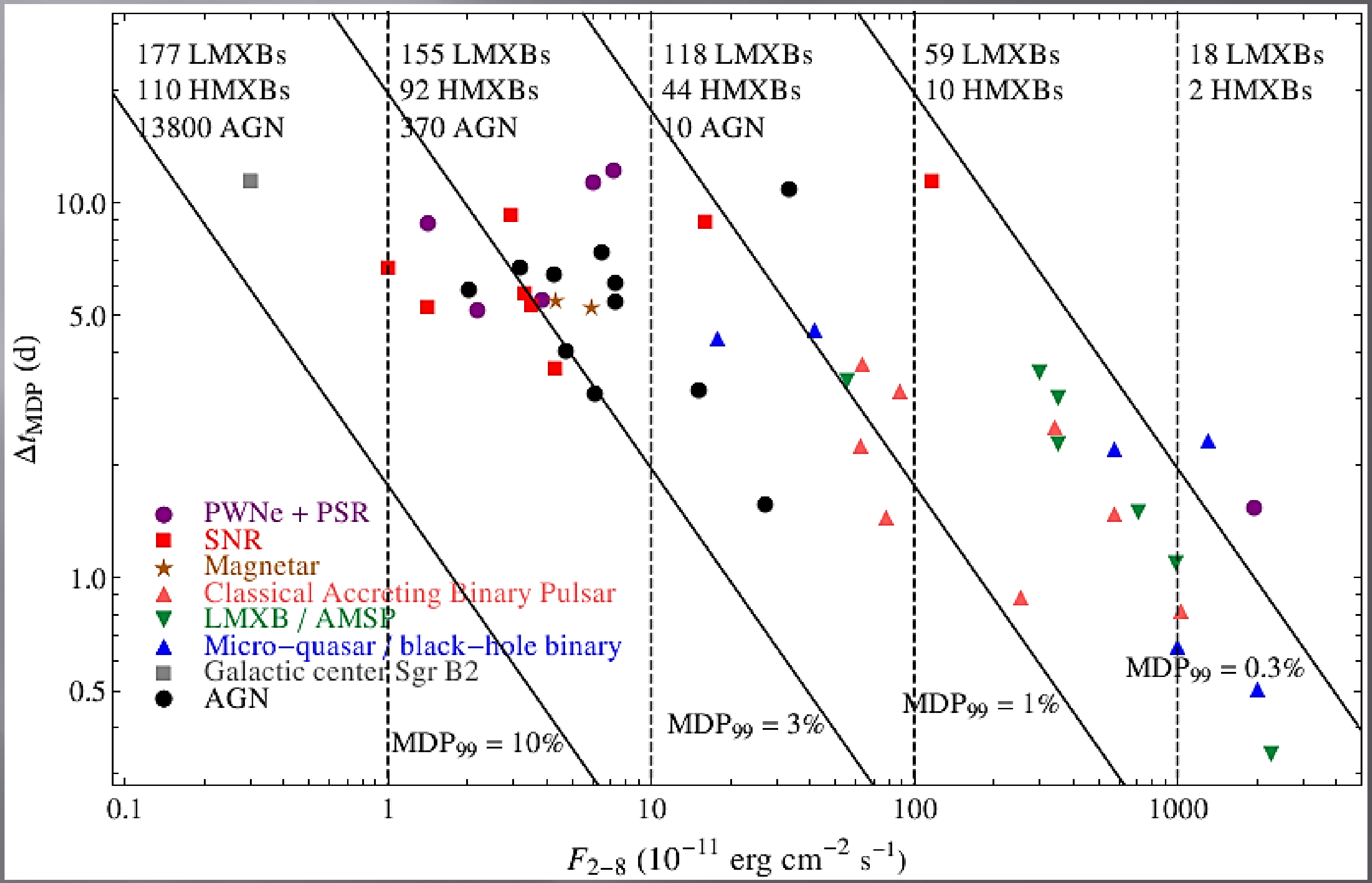

Measure black-hole spin from polarization rotation in twisted space-time

- For a micro-quasar in an accretion-dominated state
  - Scattering polarizes the thermal disk emission
  - Polarization rotation is greatest for emission from inner disk
    - Inner disk is hotter, producing higher energy X-rays
- Priors on disk orientation constrain GRX1915+105
  - model a = 0.50±0.04; 0.900±0.008; 0.99800±0.00003 (200-ks)

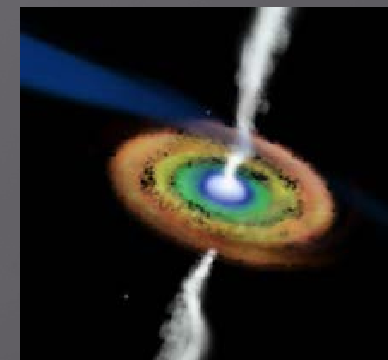

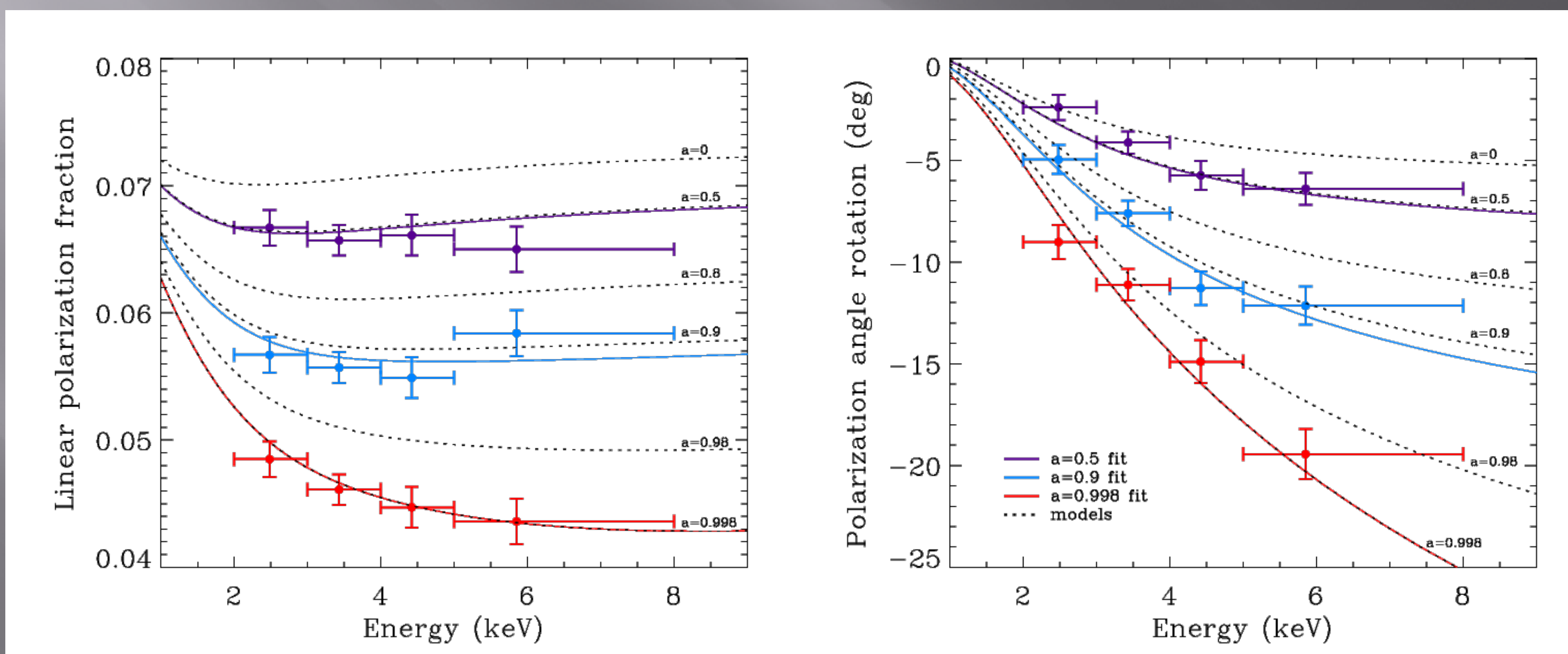

Jets in active galaxies

- **Active galaxies are powered by supermassive BHs with jets**
  - **Radio polarization implies the magnetic field is aligned with jet**
  - **Different models for electron acceleration predict different dependence in X-rays**
- **Imaging Cen A allows isolating other sources in the field**
  - **Two Ultra Luminous X-ray sources (one to SW on detector but not visible in 6-arcmin-square displayed region)**

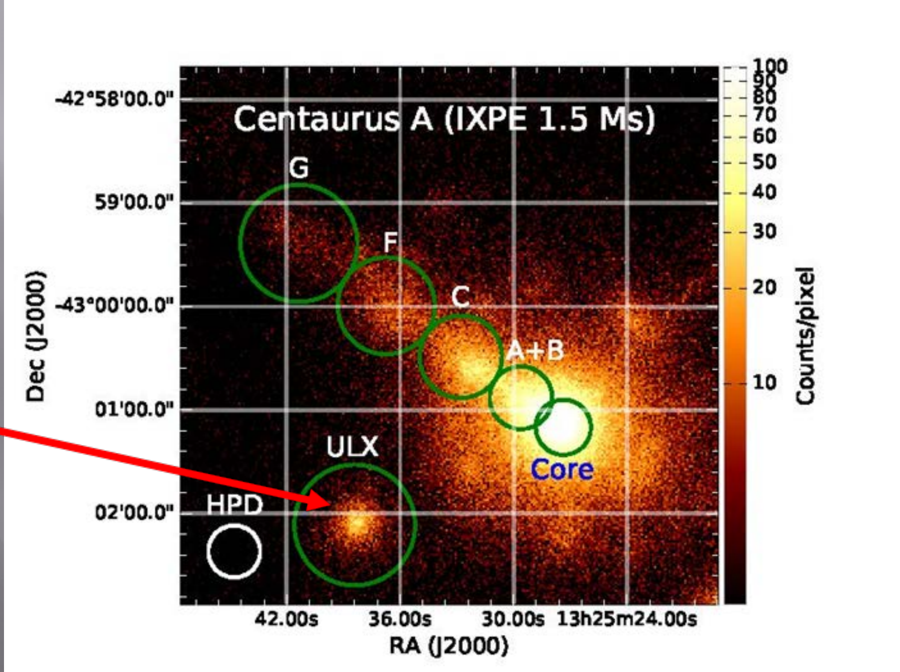

Region	MDP_{99}
Core	**<7.0%**
Jet	**10.9%**
Knot A+B	17.6%
Knot C	16.5%
Knot F	23.5%
Knot G	30.9%
ULX	**14.8%**

Includes effects of dilution by unpolarized diffuse emission

Fundamental New Measurements - Sgr A*

- **Exploit imaging polarimetry to infer past activity of Sgr A***

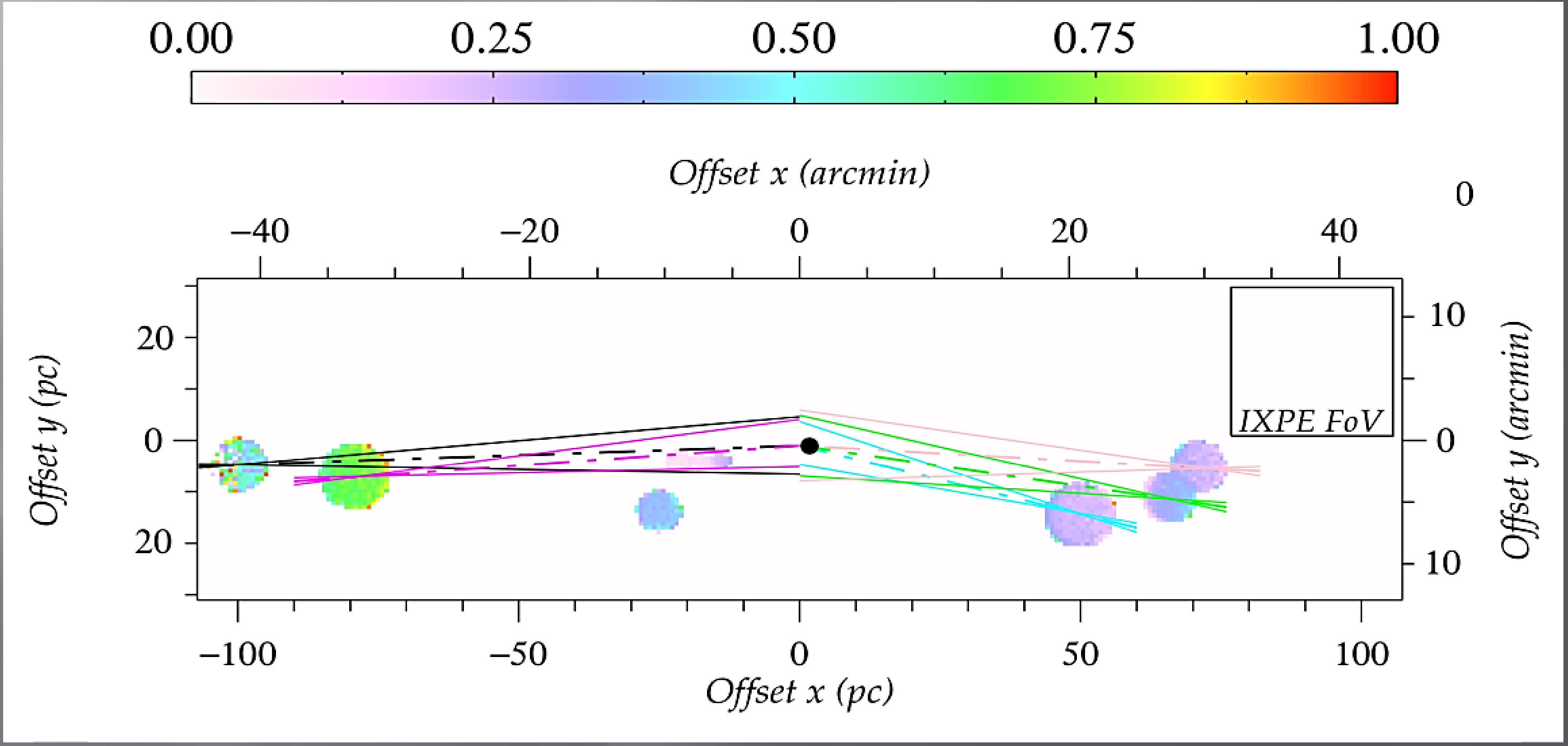

Fundamental New Measurements - PWNe

- **Map the magnetic field of X-ray-emitting regions in Pulsar Wind Nebulae**

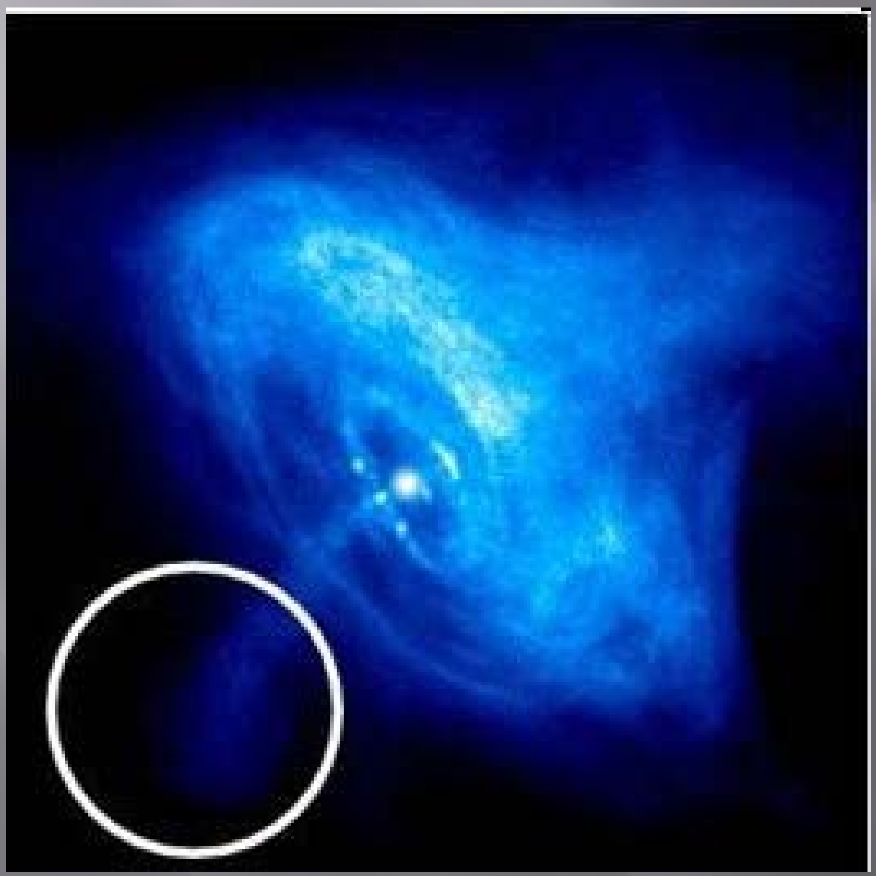

Crab

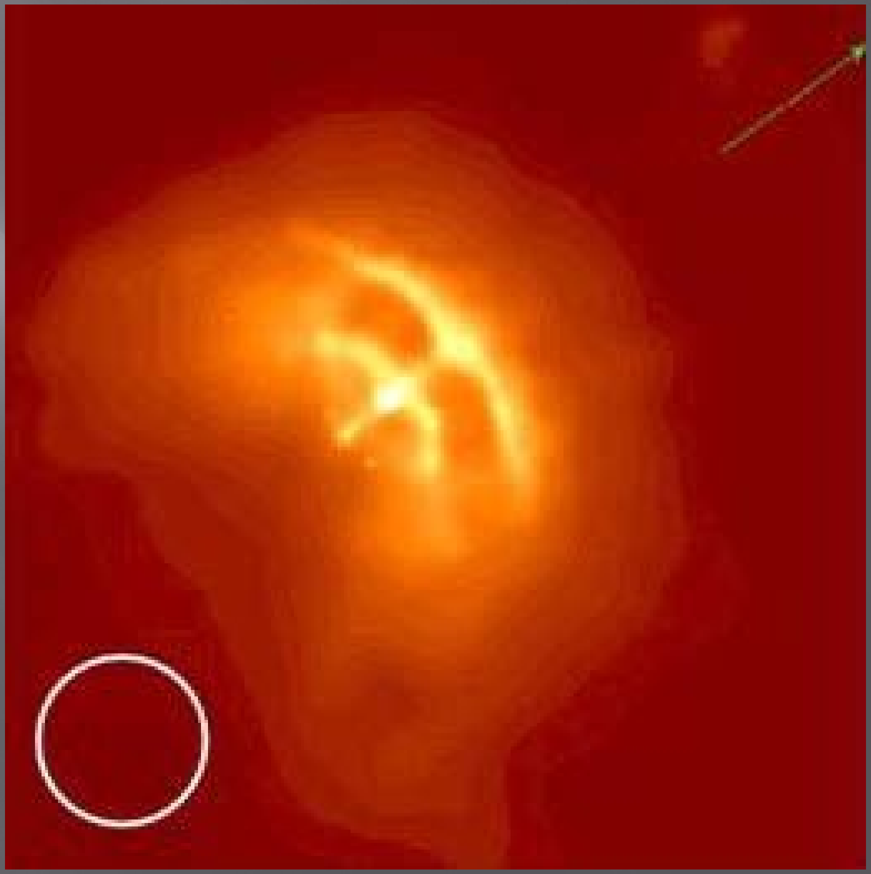

Vela

Fundamental New Measurements - PWNe

- Emission geometry and processes are unsettled
  - Competing models predict differing polarization behavior with pulse phase
- X-rays provide cleaner probe of geometry
  - Absorption likely more prevalent in visible band
  - Radiation process entirely different in radio band
    - Recently discovered no pulse phase-dependent variation in polarization degree and position angle @ 1.4 GHz
- 140-ks observation gives ample statistics to track polarization degree and position angle

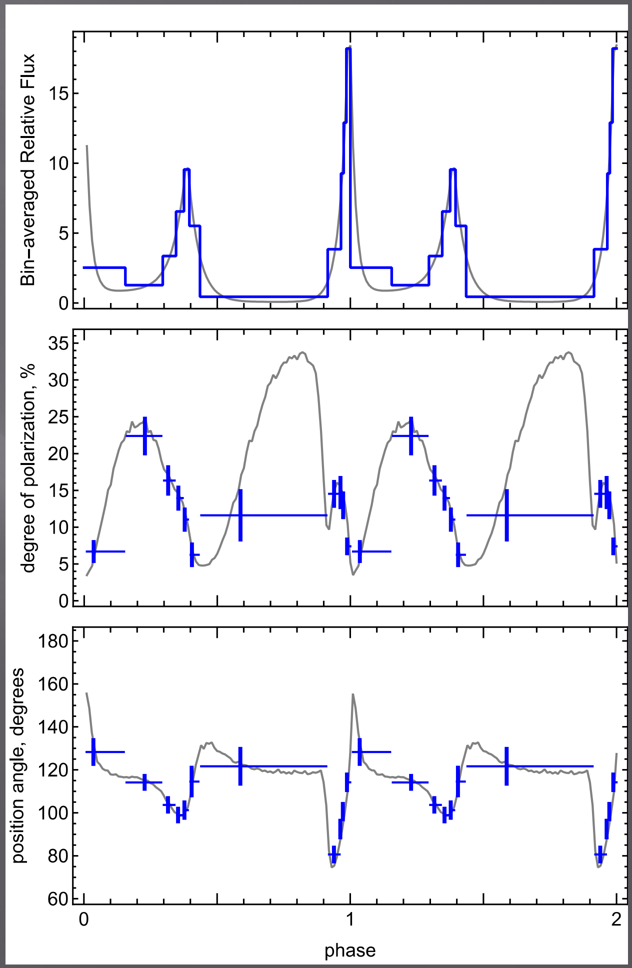

Test QED in ultra-strong magnetic fields

- **Magnetar is a neutron star with magnetic field up to 10^{15} G**
- **Non-linear QED predicts magnetized-vacuum birefringence**
  - **Refractive indices of the two polarization modes differ from 1 & each other**
  - **Impacts polarization and position angle as functions of pulse phase,**
- **Example is the magnetar 1RXS J170849.0-400910, with an 11-s pulse period where we can exclude QED-off at better than 99.9% confidence in 250-ks**

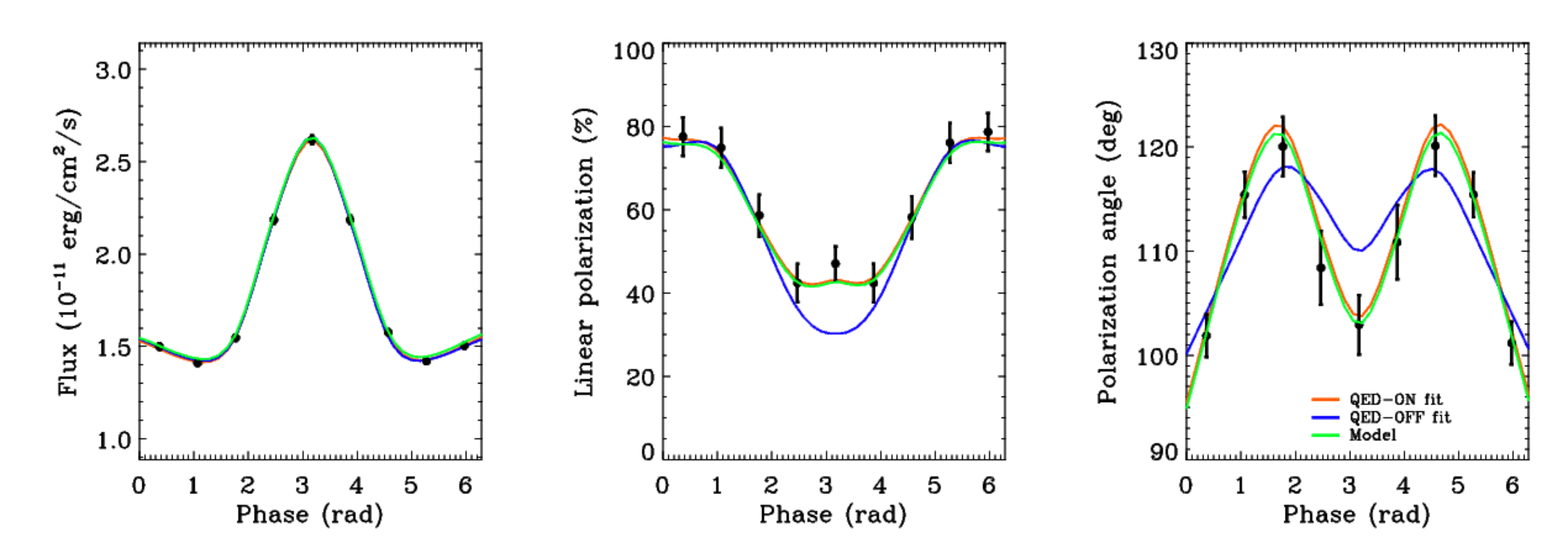

Map magnetic field of synchrotron sources

- **Lines and thermal continuum dominate @ 1-4 keV**
- **Non-thermal emission dominates @ 4-6 keV**

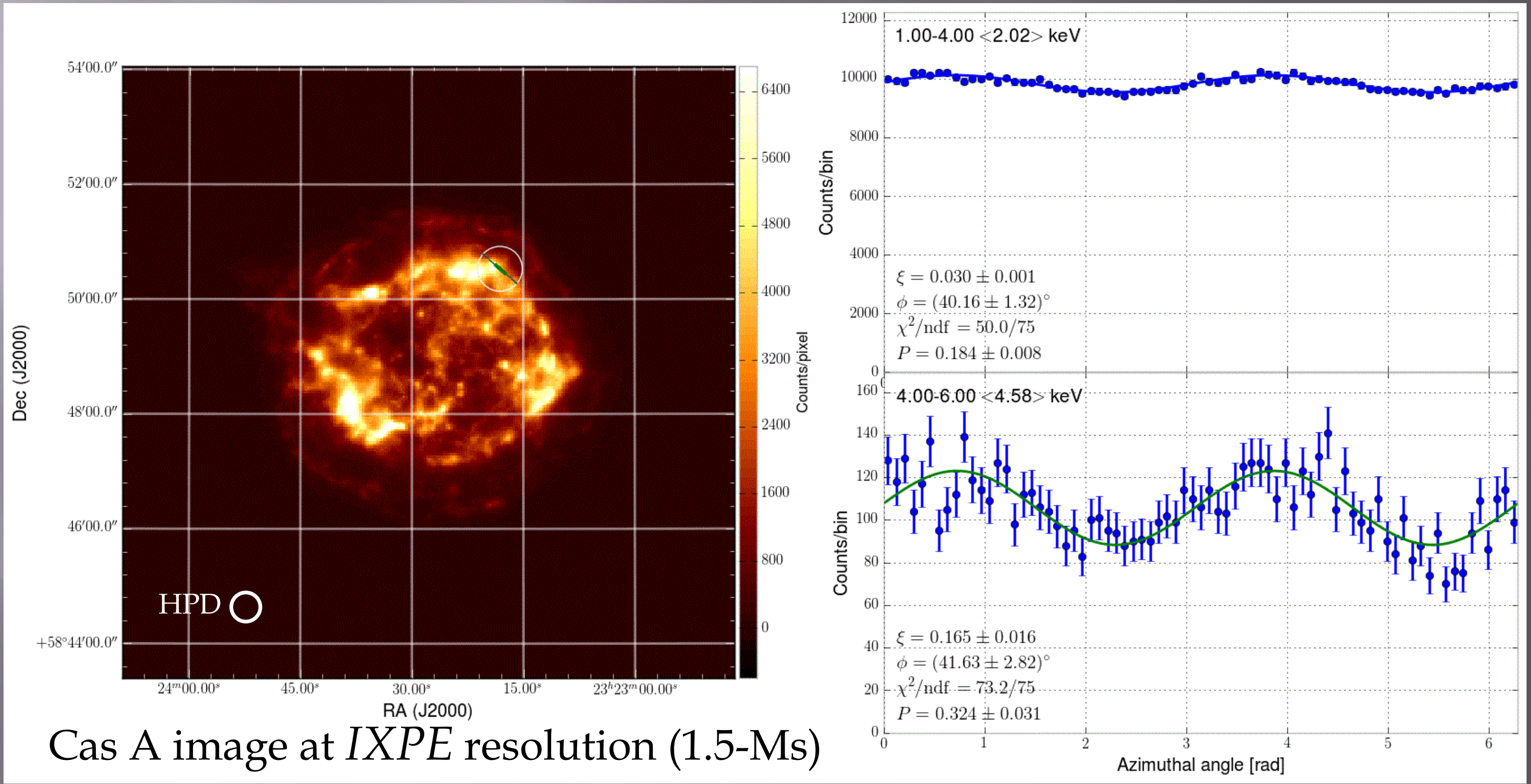

Cas A image at *IXPE* resolution (1.5-Ms)